Distribution of structure factors and phase transitions in a driven lattice gas

1996 J. Phys. A: Math. Gen. 29 6717

(http://iopscience.iop.org/0305-4470/29/21/008)

J. Phys. A: Math. Gen. **29** (1996) 6717–6728. Printed in the UK

Distribution of structure factors and phase transitions in a driven lattice gas

M S Rudzinsky† and R K P Zia‡

† Strategic and Space Systems Department, Naval Surface Warfare Center, Dahlgren Division, 17320 Dahlgren Road, Dahlgren, VA 22448-5100, USA

‡ Center for Stochastic Processes in Science and Engineering and Physics Department, Virginia Polytechnic Institute and State University, Blacksburg, VA 24061-0435, USA

Received 8 May 1996

Abstract. Using Monte Carlo methods, we study the full distribution of structure factors in the standard driven lattice gas at half filling. The time evolution of the structure factors associated with the two lowest non-trivial wavevectors is used to construct histograms. For saturation drive, at temperatures well above T_c, both are exponentially distributed, but with different widths. These results are well described by a continuum field theory with a dynamics which violates the usual fluctuation dissipation theorem. As T is lowered, one of these distributions remains essentially unaltered. By contrast, the other develops a maximum away from the origin, while staying single-peaked throughout. This behaviour is an unmistakable signal for a continuous transition.

1. Introduction

To probe a physical system, one of the most venerable techniques is to study the scattering of a beam of, e.g., light, electrons or neutrons. If there are many stochastic degrees of freedom in the system, the intensity of the scattered radiation is a direct measure of the *average* two-point correlation. The quantities involved in this correlation function differ from system to system. For example, they could be deviations of the local densities from the overall average, in case of fluid mixtures, or simply local spin densities in the case of ferromagnetic systems. Here, we refer to them collectively as $\phi(\boldsymbol{x}, t)$. Note that, in addition to the spatial coordinate $\boldsymbol{x}$, we have introduced time dependence into ϕ, since these densities clearly fluctuate in time. Depending on the set-up of the scattering experiment, the timescales associated with these fluctuations might be small or large. Often, they are small, so that a typical measurement of the intensity of the scattered beam reveals the ϕ–ϕ correlation as averages over both space and time. On the other hand, if 'snap-shots' of $\phi(\boldsymbol{x}, t)$ for different t can be stored separately, then we have the ϕ–ϕ correlation as averages over space only, while the temporal average can be taken afterwards to produce the previous result. Of course, in the latter case, we have more information about our system. For example, instead of taking the temporal average to produce the mean, we could also find the standard deviation and other statistical quantities. Indeed, we could study the entire distribution function. The 'price paid' for this extra information is that each individual 'snap-shot' appears as a random pattern of speckles. The study of such patterns and their statistical properties in laser scattering is well established [1].

0305-4470/96/216717+12$19.50

In this paper, we analyse these distributions of a *non-equilibrium steady-state* system, namely the driven diffusive lattice gas [2, 3]. Introduced by Katz *et al* [2], it is meant to capture the physics of fast ionic conductors subjected to a constant electric field. Using only the bare essential ingredients, this model consists of particles diffusing in a fixed background lattice, with hopping rates that depend on a nearest-neighbour attractive potential, an excluded volume constraint *and the external drive*. Clearly, it is one of the simplest systems for the study of statistical mechanics of non-equilibrium steady states. In the absence of the drive, this is the Ising model [4] with a constraint on its total magnetization. Many of its properties are well known, especially in two dimensions [5]. On the other hand, when driven far from equilibrium, this system displays novel collective behaviour [3]. In particular, though the second-order phase transition, for a half-filled lattice, survives at all values of the drive, its properties are quite distinct from the case in equilibrium. For example, the ordered phase develops as a result of phase segregation *transverse* to the drive only [2]. In terms of the local density, this means that *only* the transverse diffusion coefficient vanishes as T approaches T_c. By contrast, for systems in equilibrium, both coefficients are proportional to the inverse static susceptibility and must vanish together. One major consequence is that the critical properties are entirely different from those in the Ising universality class [6].

One goal of this paper is to show that distributions of the structure factor are excellent tools for studying phase transitions here. Specifically, they provide a clear signal of the second-order transition, as displayed in the lowest transverse component of the structure factor, as well as the *lack* of a major event in the longitudinal component. To obtain these distributions, we constructed histograms from the time traces of 'snap-shots' of the two-point correlations. Of course, these traces carry even more information, namely, the evolution from e.g., an initial random phase to a final phase segregated state. In the next two sections, we provide a detailed description of the model studied and the simulation results. In section 4, we analyse the macroscopic properties, using a continuum field theoretic approach. For the disordered phase, this framework is quite successful in predicting the exponential distribution observed in simulations. Finally, we summarize our findings and speculate on future studies.

2. Specifications of the model

To describe the driven diffusive lattice gas we start with the usual Ising model, defined on a d-dimensional hypercubic lattice with N sites. Each lattice site, labelled by i, can be occupied or empty. Associated with these two states is an occupation variable $n_i = 1$ or 0. Alternatively, we can describe this model in terms of spins, where the states at each site is described by $\sigma_i = \pm 1$. The relationship between these two descriptions is: $\sigma_i = 2n_i - 1$. In the following sections the spin language is used since it displays the particle–hole symmetry explicitly. A configuration, denoted by $\mathcal{C}$, is specified by either the set of occupation numbers $\{n_i\}$ or spins $\{\sigma_i\}$.

The internal energy of a configuration of this system, assuming only a nearest-neighbour interaction, is given by the Ising Hamiltonian

$$\mathcal{H} = -J \sum_{\langle i,j \rangle} \sigma_i \sigma_j \tag{2.1}$$

where the sum is over nearest-neighbour sites. We restrict ourselves to $J > 0$, corresponding to attractive (ferromagnetic) interactions. The interactions of our system with its environment are represented by a coupling to a heat bath at a temperature T.

In equilibrium, all properties can then be computed by using the canonical distribution: $\mathcal{P}_{\rm eq}(\mathcal{C}) \propto {\rm e}^{-\beta\mathcal{H}}$, where $\beta \equiv 1/k_{\rm B}T$. For $d = 2$, this system undergoes a well known second-order transition at the Onsager temperature: $2.269J/k_{\rm B}$ [5]. In the subsequent sections, all Ts will be given in units of this quantity.

Since our eventual goal is the study of non-equilibrium steady states, let us discuss first the time evolution, i.e. dynamics, of our system. In general, the lattice gas is now described by a time-dependent probability distribution $\mathcal{P}(\mathcal{C}, t)$, which satisfies a master equation:

$$\frac{\partial}{\partial t}\mathcal{P}(\mathcal{C}, t) = \sum_{\mathcal{C}'}\{W[\mathcal{C}' \to \mathcal{C}]\mathcal{P}(\mathcal{C}', t) - W[\mathcal{C} \to \mathcal{C}']\mathcal{P}(\mathcal{C}, t)\} \tag{2.2}$$

where $W[\mathcal{C} \to \mathcal{C}']$ stands for the rate at which the system makes a transition from $\mathcal{C}$ to $\mathcal{C}'$. Specifying these rates determines the model dynamics, and, jointly with the boundary conditions, the stationary distribution: $\mathcal{P}^*(\mathcal{C}) \equiv \mathcal{P}(\mathcal{C}, t \to \infty)$. For a system to reach equilibrium where $\mathcal{P}^*(\mathcal{C})$ is the canonical $\mathcal{P}_{\rm eq}(\mathcal{C})$, the rates must be chosen to satisfy the detailed balance condition:

$$\frac{W[\mathcal{C}' \to \mathcal{C}]}{W[\mathcal{C} \to \mathcal{C}']} = \frac{\mathcal{P}_{\rm eq}(\mathcal{C})}{\mathcal{P}_{\rm eq}(\mathcal{C}')}. \tag{2.3}$$

Since the right-hand side is a function of $\Delta\mathcal{H} \equiv \mathcal{H}(\mathcal{C}') - \mathcal{H}(\mathcal{C})$ only, it is possible to choose rates of the form $W[\mathcal{C} \to \mathcal{C}'] = w(\beta\Delta\mathcal{H})$, where w is any function satisfying $w(-x) = {\rm e}^x w(x)$. In our simulations, Metropolis [7] rates, i.e. $w(x) = \min\{1, {\rm e}^{-x}\}$ are used. Finally, we are interested in modelling a particle–hole system, we will choose Kawasaki's 'spin-exchange' dynamics [8], i.e. $\mathcal{C}$ and $\mathcal{C}'$ can differ by a single nearest-neighbour particle–hole exchange. We will often refer to this change of a configuration as a 'particle-hop'. Note that, as a result, the total particle number (or the total magnetization) is a constant of the motion.

Turning our focus to non-equilibrium steady states, we introduce a driving field which we label by $\boldsymbol{E}$. Its effect on the particles is to favour (suppress) hops in the direction of (against) $\boldsymbol{E}$, while transverse jumps remain unchanged. Such an external field is motivated by either a gravitational field coupled to the more massive 'particles' or by an 'electric' field coupled to 'charged' particles. In our model $\boldsymbol{E}$ is assumed to be uniform in both space and time and points along a specific lattice axis. This bias of the field can now be introduced in the Ising lattice gas by modifying the set of transition rates, $W[\mathcal{C} \to \mathcal{C}']$, to include the work done locally by the field. Thus, we add a term lE to $\Delta\mathcal{H}$ in the rate functions where $l = (-1, 0, +1)$ specifies jumps (along, transverse to, against) $\boldsymbol{E}$. Incorporating (2.3), which may be interpreted as a 'local detailed balance' condition, and using Metropolis rates, we write

$$W[\mathcal{C} \to \mathcal{C}'] = \min\{1, {\rm e}^{-[\beta(\Delta\mathcal{H}+lE)]}\} \tag{2.4}$$

where E represents the product of the magnitude of $\boldsymbol{E}$, the 'charge' of the particle, and a lattice constant. Finally, we must specify the boundary conditions. Since our interest is in establishing a *non-equilibrium* steady state, we select boundary conditions which excludes this dynamics from being derivable from a global Hamiltonian. The simplest choice is periodic boundary conditions (PBC), under which a non-trivial steady current is established globally. A further advantage is that this system respects translational invariance.

3. Simulation results

We have performed Monte Carlo simulations of the driven diffusive model described above, using 30×30 lattices ($N = 900$). This size was chosen partly because it allows a convenient

comparison with the original investigation [2]. To study the *distribution* of the structure factors, we let this system run in a steady state and measure various two-point correlations (and their Fourier transforms) at regular time intervals. From their time series, instead of finding a simple average, we build histograms which represent the distributions. The temperature is then varied, in order to study how these distributions change as the system goes through its critical point.

In the literature, the term 'structure factor', denoted by $S(\boldsymbol{k})$ here, typically refers to the (ensemble- or time-) average of the operator:

$$\hat{s}(\boldsymbol{k}) \equiv \frac{1}{N} \sum_{i,j} \mathrm{e}^{\mathrm{i}\boldsymbol{k}\cdot(j-i)} \sigma_i \sigma_j \tag{3.1}$$

i.e.

$$S(\boldsymbol{k}) = \langle \hat{s}(\boldsymbol{k}) \rangle. \tag{3.2}$$

Since $\langle \sigma_i \sigma_j \rangle$ is the spin–spin correlation function, S corresponds to its Fourier transform. As time evolves and the configuration changes in a simulation, $\hat{s}(\boldsymbol{k})$, for each specific $\boldsymbol{k}$, takes on various values. The average of these values is then reported as $S(\boldsymbol{k})$. Here, we seek the entire distribution of these values, i.e. the function

$$P(s; \boldsymbol{k}) = \langle \delta(s - \hat{s}) \rangle. \tag{3.3}$$

Since our dynamics conserves total magnetization, $\hat{s}(0)$ is fixed and its distribution is trivial. Turning to non-zero $\boldsymbol{k}$, we focus on, for simplicity, the two lowest values: one longitudinal and one transverse to $\boldsymbol{E}$. In an undriven system, $x \Leftrightarrow y$ symmetry implies that there is no extra information by studying both. In the driven case however, they are drastically different [2, 3], so that measuring both quantities can be quite revealing. In particular, in a disordered phase, these $\hat{s}$'s would be O(1). On the other hand, for an ordered system, with phase segregation into two strips, one of these would be O(N), depending on the orientation of the strips. Thus, they are good candidates for an order parameter as well. Explicitly, these two wavevectors are $(k_\perp, k_\parallel) = (2\pi/30)(0, 1)$ and $(k_\perp, k_\parallel) = (2\pi/30)(1, 0)$. Their associated $\hat{s}$'s will be denoted by $\hat{s}(0, 1)$ and $\hat{s}(1, 0)$, respectively.

For our simulations, we set E at $50J$, which corresponds to, for all practical purposes, an 'infinite' drive. The reason for this choice is to maximize the difference between a non-equilibrium system and its equilibrium counterpart. With such a large drive, it is known that the driven model, at half filling, undergoes a second-order phase transition at $T_\mathrm{c} \simeq 1.4$ [9]. Thus, we will examine a range of temperatures from $T = 2.2$ to 1.2, in steps of 0.2.

The initial configurations of each run are random and half-filled, corresponding to total magnetization of zero ($\sum \sigma_i = 0$). Quenching to $T = 2.2$, we then let the system run for 100 K Monte Carlo steps (MCS). Starting with this final configuration, T is lowered by 0.2 and the system is run for another 100 K MCS. This procedure is repeated until T reaches 1.2. After each quench, measurements were not taken during the first 10 K MCS, so that the system may settle down to the new steady state. Data for $\hat{s}(1, 0)$ and $\hat{s}(0, 1)$ are then collected by sampling configurations every 100 MCS. Thus, each of these time traces contain 900 points. Finally, to insure an adequate data sample near T_c, we have taken the last configuration of the $T = 1.4$ run and let the system evolve for another 100 K MCS. As a result histograms for this T are built from 1900 data points.

In figures 1(a)–(c), we show the time traces of $\hat{s}(1, 0)$ for three different temperatures: $T = 2.2$, 1.4 and 1.2, respectively. Clearly, $\hat{s}(1, 0)$ indicates that ordering, associated with strips aligned with the field, occurred. With these traces, and similar ones for $\hat{s}(0, 1)$, we select appropriate bin sizes (on the vertical axis) to construct histograms. Thus, a histogram

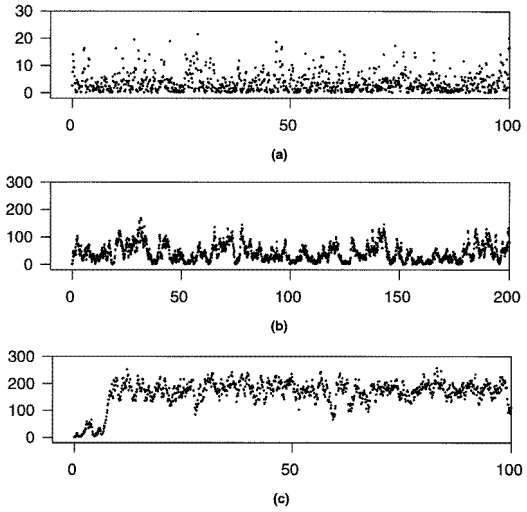

Figure 1. Time traces of $\hat{s}(1,0)$ for three different temperatures. The unit of time is 10^3 MCS. (a) $T = 2.2$, (b) $T = 1.4$, (c) $T = 1.2$.

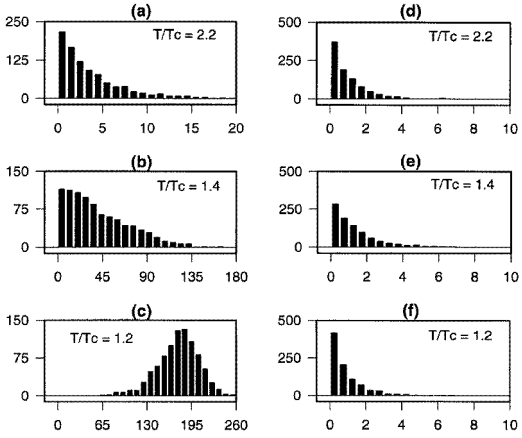

Figure 2. Histograms representing distributions of structure factors, $P(s;\boldsymbol{k})$. Figures in the left column (a)–(c) are for $\hat{s}(1,0)$. Those in the right column (d)–(f) are for $\hat{s}(0,1)$.

displays, effectively, the horizontal cross sections of a time trace. In figure 2 we show such histograms for both $\hat{s}(1,0)$ and $\hat{s}(0,1)$, at the same three Ts. Note that the bin size for $\hat{s}(0,1)$ is fixed at 0.5. However, since $\hat{s}(1,0)$ increases through the phase transition we use an increasing bin size to display these distributions, i.e. 1, 8, and 10 for $T = 2.2$, 1.4, and 1.2, respectively. Similarly, note that the scale of the abscissae are not uniform throughout, further highlighting the contrast between the two structure factors. Finally, to match the other cases, we have renormalized the $T = 1.4$ histograms, since there are more than twice the number of data points here.

The most striking feature displayed in figure 2 is surely the contrast between the behaviour of $\hat{s}(1,0)$ and $\hat{s}(0,1)$. As T drops through the transition, the distribution for the latter shows almost imperceptible changes. On the other hand, the distribution for

$\hat{s}(1,0)$, while displaying significant changes, remains *single-peaked* throughout. This is a clear signal of a continuous transition. In particular, at $T = 1.4$, the slope of the distribution at the origin is zero, which is consistent with the assignment of a second-order transition. The extent of the fluctuations can also be appreciated directly: from very large values for $\hat{s}(1,0)$ near or below criticality, to O(1) for $\hat{s}(0,1)$ at all T and $\hat{s}(1,0)$ in the disordered phase. A more thorough study of the critical region, in the spirit of those for the equilibrium Ising model [10], should be carried out, with the most likely outcome being a universal scaling distribution. In this paper, we focus on the distributions for $T \gg T_c$. These turn out to be exponentials. In figure 3, log-linear plots of the distributions for both $\hat{s}$'s, at $T = 2.2$, show that the data points generally fall on a straight line. Least-squares fits with straight lines are then used to yield the slopes. If the distributions were precisely exponential, i.e.

$$P(s;\boldsymbol{k}) \propto \mathrm{e}^{-s/s_0(\boldsymbol{k})} \tag{3.4}$$

the average would be the inverse of this slope, i.e. $s_0(\boldsymbol{k})$. Thus a comparison between the fitted slopes and the measured averages, i.e. $S(\boldsymbol{k})$ from (3.2, 3.3), will provide a crude estimate for how good the exponential approximation is. Table 1 summarizes this comparison. There is reasonably good agreement, i.e. a few per cent, between $S(\boldsymbol{k})$ and $s_0(\boldsymbol{k})$. Note that we have included some cases for near and below criticality for completeness, though we have no theoretical basis for P being an exponential. In the next section, we will provide a framework which should be valid far above the critical temperature and which predicts exponential distributions.

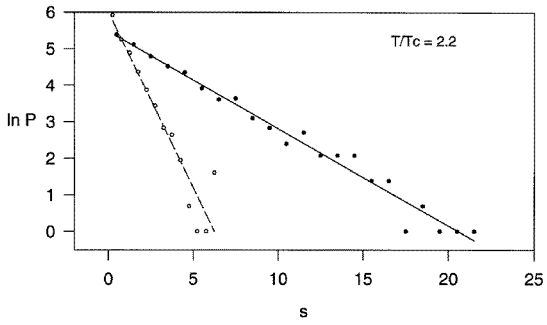

Figure 3. Plots of $\ln P(s;\boldsymbol{k})$ against s at $T = 2.2$ for $\hat{s}(1,0)$ and $\hat{s}(0,1)$ with least-squares fitted straight lines. Full circles are for $\hat{s}(1,0)$, open circles for $\hat{s}(0,1)$.

4. Analytic approach and discussion

To arrive at some understanding of the large distance behaviour found above, it is customary to exploit a coarse-grained, continuum description. The occupation numbers n_i at discrete times are replaced by a density field $\rho(\boldsymbol{x},t)$, for which a Langevin equation of motion is postulated. The simplest approach [3] begins with the continuity equation $\partial_t\rho + \boldsymbol{\nabla}\cdot\boldsymbol{J} = 0$ and writing the current as a sum of a diffusive part and an Ohmic term. The former may be chosen to be that for model B, following Hohenberg and Halperin [11]: $-\lambda\boldsymbol{\nabla}(\delta\mathcal{H}/\delta\rho)$, where λ is a (constant) transport coefficient and $\mathcal{H}$ is the free energy functional, assumed to be the Landau–Ginzburg Hamiltonian here. For the latter, we write $\mathcal{M}\mathcal{E}\hat{e}$, where $\hat{e}$ is a unit vector in the field direction, $\mathcal{E}$ is a coarse-grained version of the microscopic drive E and $\mathcal{M}$ is a (density-dependent) mobility factor which we will assume to take the simple

Table 1. Summary and comparison of (averaged) structure factors, $S(\boldsymbol{k})$ and the inverse slope $s_0(\boldsymbol{k})$, computed by two different methods for $T = 2.2$ to 1.2. '$S()$' column is the average value of the structure factor calculated directly from the time series. '$s_0()$' column is the value of the structure factor calculated from the slope of the fitted line from the ln plot of $P(s; \boldsymbol{k})$ against s.

T/T_c	$S(1, 0)$	$s_0(1, 0)$	$S(0, 1)$	$s_0(0, 1)$
2.2	3.69	3.76	1.02	1.04
2.0	5.28	5.25	1.01	1.06
1.8	6.64	6.86	1.13	1.12
1.6	12.24	12.85	1.17	1.16
1.4	45.08	—	1.29	1.27
1.2	175.07	—	0.88	0.93

form $\rho(1-\rho)$ [3]. In general, the drive will induce spatial anisotropy, so that parameters associated with the directions transverse to the field should be different from those for the 'longitudinal' direction. In addition to the above two systematic currents, there would be the random, noisy Langevin terms. Mindful of anisotropy, we denote the transverse and longitudinal components separately, by ξ_i and ζ, respectively. Both are assumed to be Gaussians, with zero mean and the following variances:

$$\langle \xi_i(\boldsymbol{x}, t)\xi_j(\boldsymbol{x}', t')\rangle = n_\perp \delta_{ij}\delta(\boldsymbol{x}-\boldsymbol{x}')\delta(t-t') \tag{4.1a}$$

and

$$\langle \zeta(\boldsymbol{x}, t)\zeta(\boldsymbol{x}', t')\rangle = n_\parallel \delta(\boldsymbol{x}-\boldsymbol{x}')\delta(t-t'). \tag{4.1b}$$

Thus, we write

$$P(\boldsymbol{\xi}, \zeta) \propto \exp\left\{-\frac{1}{2}\int \mathrm{d}\boldsymbol{x}\,\mathrm{d}t\left(\frac{\boldsymbol{\xi}^2}{n_\perp}+\frac{\zeta^2}{n_\parallel}\right)\right\} \tag{4.2}$$

for the distribution.

Putting all these terms together and using $\phi \equiv 2\rho - 1$ in the magnetic language, we arrive at [6, 3]

$$\frac{\partial}{\partial t}\phi = \lambda\left\{(\tau_\perp - \alpha_\perp\nabla^2)\nabla^2\phi + (\tau_\parallel - \alpha_\parallel\partial^2)\partial^2\phi - 2\alpha_x\partial^2\nabla^2\phi + \frac{u}{3!}(\nabla^2\phi^3 + \kappa\partial^2\phi^3)\right\} + \mathcal{E}\partial\phi^2 - (\boldsymbol{\nabla}\cdot\boldsymbol{\xi} + \partial\zeta) \tag{4.3}$$

where the *transverse gradients* have been denoted by $\boldsymbol{\nabla}$ and the longitudinal ones by ∂. All these parameters (including τ, α, u, κ) may be derived, in principle [12], from the microscopic model. Thus, they should be regarded as functions of J, E and T, just as the parameters in a Landau–Ginzburg Hamiltonian would be functions of those in the microscopic system. While the details of these functions are not needed for predicting macroscopic phenomena, a few basic properties must be established.

First, we focus on the τ's and n's. If we were describing an equilibrium system with anisotropic couplings and/or anisotropic transport coefficients, we must impose detailed balance. One of its consequences is the fluctuation dissipation theorem (FDT), which, in this case, implies the constraint $\tau_\perp/\tau_\parallel = n_\perp/n_\parallel$. However, our interest is a system in non-equilibrium steady state, so that we expect, generically,

$$\frac{\tau_\perp}{\tau_\parallel} \neq \frac{n_\perp}{n_\parallel}. \tag{4.4}$$

For systems in equilibrium, the τ's are associated with the inverse susceptibility above criticality, so that they must be identical and vanish as $T \to T_c$. Below T_c, it is customary

to choose $\tau < 0$, which leads to phase separation [13]. Here, there is no such constraint and they must be chosen so as to reproduce, at least qualitatively, what is observed. In simulations below criticality, only states with inhomogeneities *transverse* to $\boldsymbol{E}$ have been seen, so that it is natural to choose

$$\tau_{\parallel} > 0 \qquad \text{and} \qquad \tau_{\perp} < 0 \tag{4.5}$$

for describing the system below T_c. On the other hand, both $n_{\parallel}$ and $n_{\perp}$, being variances of noise currents, must remain positive. As for the other parameters (λ, α's, u, κ, and $\mathcal{E}$), we do not expect any changes in sign, as J, E, and T are varied, so that there should be no qualitative changes in macroscopic properties.

To proceed, in principle we would solve (4.3) for $\phi(\boldsymbol{x}, t)$, with appropriate initial conditions and then carry out the averages over $(\boldsymbol{\xi}, \zeta)$ using (4.2). In practice, however, this procedure is clearly prohibitive, except in a linear approximation. For describing our system away from criticality, renormalization group arguments show that such an approximation can be better and better, as we focus on longer and longer length scales. In particular, we will demonstrate that, for the driven system above T_c, this approach leads to exponential distributions of the structure factors, such as those reported above.

Restricting ourselves to the disordered phase in *steady state*, where $\langle\phi\rangle = 0$, we linearize (4.3) to

$$\frac{\partial}{\partial t}\phi(\boldsymbol{x}, t) = \lambda\{(\tau_{\perp} - \alpha_{\perp}\nabla^2)\nabla^2\phi + (\tau_{\parallel} - \alpha_{\parallel}\partial^2)\partial^2\phi - 2\alpha_{\mathrm{x}}\partial^2\nabla^2\phi\} - (\boldsymbol{\nabla}\cdot\boldsymbol{\xi} + \partial\zeta). \tag{4.6}$$

Defining Fourier transforms for the field and noise by $\phi(\boldsymbol{k}, \omega) \equiv \int \exp[-\mathrm{i}(\boldsymbol{k}\cdot\boldsymbol{x} + \omega t)]\phi(\boldsymbol{x}, t)$, etc, the solution to this equation is simply

$$\phi(\boldsymbol{k}, \omega) = \{\mathrm{i}\omega + \Lambda(\boldsymbol{k})\}^{-1}(-\mathrm{i})\{\boldsymbol{k}_{\perp}\cdot\boldsymbol{\xi}(\boldsymbol{k}, \omega) + k_{\parallel}\zeta(\boldsymbol{k}, \omega)\} \tag{4.7}$$

where

$$\Lambda(\boldsymbol{k}) \equiv \lambda\{\tau_{\perp}k_{\perp}^2 + \tau_{\parallel}k_{\parallel}^2 + (\alpha_{\perp}k_{\perp}^4 + 2\alpha_{\mathrm{x}}k_{\parallel}^2k_{\perp}^2 + \alpha_{\parallel}k_{\parallel}^4)\}. \tag{4.8}$$

Since $\langle\boldsymbol{\xi}\rangle = \langle\zeta\rangle = 0$, we immediately recover $\langle\phi\rangle = 0$. Similarly, the *dynamic* structure factor can be easily obtained:

$$S(\boldsymbol{k}, \omega) \equiv \langle\phi^*(\boldsymbol{k}, \omega)\phi(\boldsymbol{k}, \omega)\rangle = \frac{N(\boldsymbol{k})}{\omega^2 + \Lambda^2(\boldsymbol{k})} \tag{4.9}$$

where

$$N(\boldsymbol{k}) \equiv n_{\perp}k_{\perp}^2 + n_{\parallel}k_{\parallel}^2. \tag{4.10}$$

From (4.9), we can find the *steady-state* structure factor $S(\boldsymbol{k})$, defined to be the equal-time correlation,

$$S(\boldsymbol{k}) \equiv \langle\phi^*(\boldsymbol{k}, t)\phi(\boldsymbol{k}, t)\rangle = \int \frac{\mathrm{d}\omega}{2\pi} S(\boldsymbol{k}, \omega) = N/2\Lambda. \tag{4.11}$$

It is the analogue of the static structure factor for equilibrium systems. Note that, for those cases, the FDT will imply more than just $\tau_{\perp}/\tau_{\parallel} = n_{\perp}/n_{\parallel}$. There would be further constraints on the α's, as well as $n \propto \lambda T$, so that $S(\boldsymbol{k})$ will take the Ornstein–Zernike form $T/(\tau + k^2)$.

Returning to driven systems, here we are interested in more than the simple average $\langle\phi^*(\boldsymbol{k}, t)\phi(\boldsymbol{k}, t)\rangle$. We seek the *entire distribution* of

$$\hat{s}(\boldsymbol{k}) \equiv \phi^*(\boldsymbol{k}, t)\phi(\boldsymbol{k}, t) \tag{4.12}$$

i.e. the function

$$P(s;\boldsymbol{k}) = \langle \delta(s-\hat{s}) \rangle = \int \mathcal{D}\boldsymbol{\xi}\mathcal{D}\zeta\, P(\boldsymbol{\xi},\zeta)\delta(s-\hat{s}). \tag{4.13}$$

Note that (4.12) is just the continuum version of (3.1). Here, we have used slightly different notation to distinguish functional integrals (over the noise here) from ordinary integrals.

Now, for each $\boldsymbol{k}$, there is such a distribution. However, at the level of the linear approximation, the $\boldsymbol{k}$-dependence of ϕ is trivially related to that of $(\boldsymbol{\xi},\zeta)$. Indeed, inverting (4.7), we have explicitly

$$\phi(\boldsymbol{k},t) = \int_{-\infty}^{t} \mathrm{d}t' \exp[-\Lambda(\boldsymbol{k})(t-t')](-\mathrm{i})\{\boldsymbol{k}_\perp \cdot \boldsymbol{\xi}(\boldsymbol{k},t') + k_\parallel \zeta(\boldsymbol{k},t')\}. \tag{4.14}$$

Meanwhile, $\delta(s-\hat{s})$ depends on only ϕ and ϕ^*, the latter being $\phi(-\boldsymbol{k},t)$ due to the reality of $\phi(\boldsymbol{x},t)$. Thus, it is a function of 'monochromatic' (i.e., a single pair of $\boldsymbol{k}'$ and $-\boldsymbol{k}$) noise. Inspecting (4.2), we see that $P(\boldsymbol{\xi},\zeta)$ is also Gaussian in $\boldsymbol{\xi}(\boldsymbol{k},t)$ and $\zeta(\boldsymbol{k},t)$, so that it factorizes into products over 'monochromatic' Gaussians. Thus, all integrations in (4.13) are trivial, except those associated with a *single pair*: $\pm\boldsymbol{k}$. As a result, we can regard

$$\mathcal{D}\boldsymbol{\xi}\mathcal{D}\zeta \qquad \text{as} \qquad \prod_t \mathrm{d}\boldsymbol{\xi}(\boldsymbol{k},t)\,\mathrm{d}\boldsymbol{\xi}(-\boldsymbol{k},t)\,\mathrm{d}\zeta(\boldsymbol{k},t)\,\mathrm{d}\zeta(-\boldsymbol{k},t). \tag{4.15}$$

A convenient way to deal with the pair is to use, e.g.,

$$\mathrm{d}\boldsymbol{\xi}(\boldsymbol{k},t)\,\mathrm{d}\boldsymbol{\xi}(-\boldsymbol{k},t) = \mathrm{d}\boldsymbol{\xi}(\boldsymbol{k},t)\,\mathrm{d}\boldsymbol{\xi}^*(\boldsymbol{k},t) \tag{4.16}$$

so that, once a particular $\boldsymbol{k}$ is chosen through (4.12), we can ignore $-\boldsymbol{k}$ completely. At this stage, regarding $\boldsymbol{k}$ as a parameter and dropping all explicit reference to it would be most natural. However, the exponent in $P(\boldsymbol{\xi},\zeta)$ involves an integral over all momenta, so that it will contain, e.g., $|\boldsymbol{\xi}(\boldsymbol{k},t)|^2/n_\perp$ as well as $|\boldsymbol{\xi}(-\boldsymbol{k},t)|^2/n_\perp$. Since the latter is identical to the former, we may simply double the integral and write

$$P(\boldsymbol{\xi},\zeta) \propto \exp\left\{ -\int \mathrm{d}t \left(\frac{|\boldsymbol{\xi}(t)|^2}{n_\perp} + \frac{|\zeta(t)|^2}{n_\parallel} \right) \right\}. \tag{4.17}$$

To go further, we find it easier to study the Laplace transform of (4.13):

$$\tilde{P}(\mu) = \int \mathrm{d}s\, P(s)\, \mathrm{e}^{-\mu s} = \int \mathcal{D}\boldsymbol{\xi}\mathcal{D}\zeta\, P(\boldsymbol{\xi},\zeta) \exp(-\mu\hat{s}). \tag{4.18}$$

Inserting (4.14) into (4.12), we see that $\hat{s}$ is also quadratic in the noise, though diagonal in neither the component index nor t. Thus, the integrand in (4.18) is still a Gaussian, controlled by the quadratic form:

$$\eta_\alpha^* \{ D_{\alpha\beta} + \mu v_\alpha^* v_\beta \} \eta_\beta \tag{4.19}$$

where we have combined all components of the noise into η and used α to denote both the component index and t ('sum' over t means $\int \mathrm{d}t$). Here, D is diagonal, e.g., $\delta(t-t')\delta_{ij}/n_\perp$ for the transverse components. Meanwhile, v can be read from (4.14):

$$v_i(t') = -\mathrm{i}(\boldsymbol{k}_\perp)_i\, \mathrm{e}^{-\Lambda(t-t')}\Theta(t-t') \qquad \text{and} \qquad v_\parallel(t') = -\mathrm{i}k_\parallel\, \mathrm{e}^{-\Lambda(t-t')}\Theta(t-t') \tag{4.20}$$

where Θ is the step function. Since the η's are complex and the matrix in (4.19) is Hermitian, the Gaussian integrals lead to determinants rather than their square roots. Thus, (4.18) can be evaluated:

$$\tilde{P}(\mu) = \det\{D_{\alpha\beta}\} / \det\{D_{\alpha\beta} + \mu v_\alpha^* v_\beta\} \tag{4.21}$$

where the numerator comes from the normalization factor (so that $\tilde{P}(0) = 1$).

The inverse of D is well defined, given that it represents the noise correlation, so that (4.21) reduces to $1/\det\{\delta_{\alpha\beta} + \mu D^{-1}_{\alpha\gamma} v^*_\gamma v_\beta\}$. But, $\det\{\delta_{\alpha\beta} + a^*_\alpha b_\beta\} = 1 + a^*_\alpha b_\alpha$, leading us to

$$\tilde{P}(\mu) = 1/\{1 + \mu v^*_\alpha D^{-1}_{\alpha\beta} v_\beta\}. \tag{4.22}$$

Explicitly, $v^* D^{-1} v$ is just

$$\int_{-\infty}^{0} \mathrm{d}t' \, \mathrm{d}t'' \, \mathrm{e}^{\Lambda t'} \delta(t' - t'') \{n_\perp k_\perp^2 + n_\parallel k_\parallel^2\} \, \mathrm{e}^{\Lambda t''} \tag{4.23}$$

which is just $N/2\Lambda$, i.e. $S(\boldsymbol{k})$ as defined in (4.11). Inserting this into (4.22) and inverting the Laplace transform, we have

$$P(s; \boldsymbol{k}) \propto \exp(-s/S(\boldsymbol{k})) \tag{4.24}$$

i.e. an exponential distribution.

One important consequence of (4.24) is that its standard deviation, $\sqrt{\langle(\hat{s} - S)^2\rangle}$, takes *the same value as* the average. For those unfamiliar with distribution of laser speckles, say, to find such a result may seem alarming. Naively, our confidence in a statistical sample would be greater if the standard deviation, compared to the average, is smaller. Here, as (4.24) shows, the better the sample, the closer the two will be.

For temperatures far above T_c, the linear approximation (4.6) should be good and, as shown in figure 3, the histograms fit the exponential quite well. Not surprisingly, the inverse slopes extracted from linear fits to these plots agree with the averages $\langle\phi^*\phi\rangle$. Though we have presented the results for only two momenta, we have collected data for a few other cases, with similar conclusions. However, for larger $\boldsymbol{k}$, the correlations are smaller and the statistics are correspondingly poorer.

As T_c is approached, the analysis above, based on a linear approximation about $\langle\phi\rangle = 0$, is expected to fail. This breakdown is clearly seen in figure 2(b), for which (4.24) is very far from being a good fit. In fact, the distribution is reminiscent of a Gaussian! Perhaps surprising, this resemblance can be understood qualitatively. Since the structure factor is the product of a pair of ϕ's, a Gaussian in $\hat{s}$ would be similar to $\exp(-\phi^4)$. Similarly, if we used Landau theory for the Ising model at criticality, and plotted the resultant against M^2 instead of M, we would also have a Gaussian. Returning to the histogram, we see that the slope in the neighbourhood of $\hat{s}(1, 0) = 0$ vanishes, which supports the phenomenological choice $\tau_\perp \to 0$ as a description of $T \to T_c$. To carry out a reliable analysis for $T \simeq T_c$ would require not only the full power of dynamic renormalization group [6, 14], but also generalizations to include terms like $-\mu\hat{s}(\boldsymbol{k}) = -\mu\phi^*(\boldsymbol{k}, t)\phi(\boldsymbol{k}, t)$ in the dynamic functional. This highly non-trivial undertaking would be worthwhile, but is beyond the scope of this paper. Turning to the histogram for $\hat{s}(0, 1)$ (figure 2(e)), it does not appear to differ much from an exponential. If we used mean-field theory alone, we would argue that this is consistent with choosing $\tau_\parallel > 0$ throughout the critical region. However, since it is known that $\langle\hat{s}(0, 1)\rangle$ suffers non-trivial renormalization [6], we should expect this distribution to be modified by fluctuations also. Nevertheless, these effects may be quantitatively small, leading to the close resemblance of the data to (4.24). Again, before a careful renormalization analysis, sharp conclusions should not be drawn.

Below criticality, we see that the distribution of $\hat{s}(1, 0)$ is no longer peaked about the origin (figure 2(c)), a clear confirmation of its role as the appropriate order parameter. To carry out the theoretical analysis for this is also no simple task. Indeed little or no analytic work has been done on the details of the coexistence curve [3]. Finally, the histogram for $\hat{s}(0, 1)$ here (figure 2(f)) also appears to be an exponential. Since it is not the order

parameter, perhaps it is possible to carry out the analysis, as in the $T \gg T_c$ cases. We believe that this is the most promising direction for progress in the immediate future.

To summarize, we have presented histograms of Monte Carlo data for the two most important structure factors in the standard driven lattice gas [2, 3], namely $\hat{s}(1, 0)$ and $\hat{s}(0, 1)$, corresponding to the transverse and longitudinal components of the lowest wavevectors. At infinite drive and T well above T_c, both are exponentially distributed, but controlled by different parameters. These aspects are well described by a continuum field theory with an FDT-violating dynamics, linearized about the half-filled disordered state. As T_c is approached, the distribution of the transverse component flattens out to resemble a Gaussian. Below criticality, the peak gradually moves away from the origin, which is the hallmark of a second-order transition. Meanwhile, the histograms for $\hat{s}(0, 1)$ remain sharply peaked at the origin throughout the transition. Though there may be non-trivial renormalization effects, they appear to be small, lending much confidence to (4.5) being the appropriate starting point for a field theory for $T \lesssim T_c$.

For future work, a number of lines of attack present themselves clearly. Our histograms may be regarded as generalizations of those investigated by Binder [10] for the total magnetization in the non-conserved Ising model. In that case, a much deeper understanding of the critical properties ensued, e.g., universal cumulant ratio and distribution [10, 15]. For the non-equilibrium system, only the cumulant ratio has been used extensively in simulation studies [9]. Extension to include the entire distribution would be desirable, an undertaking which will involve several anisotropic lattices [9]. On the theoretical front, a complete theory of finite size effects, along the lines of [15], would give us a much clearer picture of the universal behaviour. Beyond these, questions about the ordered state naturally arise. Simulations of systems away from half-filling [16] with various lattices should be performed systematically so as to map out the co-existence curve more reliably. Finally, we can point to the large variety of non-equilibrium steady states [3] to which we can apply the methods of histograms.

Acknowledgments

We thank J R Heflin, G Indebetouw, B Schmittmann and M Sutton for illuminating discussions. One of us (MSR) would like to thank the System Engineering and Analysis Branch for continued support. This research is supported in part by a grant from the National Science Foundation through the Division of Materials Research.

References

[1] Dainty J C 1984 *Laser Speckle and Related Phenomena* 2nd edn (Berlin: Springer)
[2] Katz S, Lebowitz J L and Spohn H 1983 *Phys. Rev.* B **28** 1655; 1984 *J. Stat. Phys.* **34** 497. For a recent review, see [3]
[3] Schmittmann B and Zia R K P 1995 *Phase Transitions and Critical Phenomena* ed C Domb and J L Lebowitz (London: Academic) vol 17
[4] Ising E 1925 *Z. Phys.* **31** 253
[5] McCoy B M and Wu T T 1973 *Two Dimensional Ising Model* (Cambridge, MA: Harvard University Press)
[6] Janssen H K and Schmittmann B 1986 *Z. Phys.* B **64** 503
Leung K-t and Cardy J L 1986 *J. Stat. Phys.* **44** 567
[7] Metropolis N, Rosenbluth A W, Rosenbluth M M, Teller A H and Teller E 1953 *J. Chem. Phys.* **21** 1087
[8] Kawasaki K 1972 *Phase Transitions and Critical Phenomena* vol 2, ed C Domb and M S Green (New York: Academic)
[9] Leung K-t 1991 *Phys. Rev. Lett.* **66** 453; 1992 *Int. J. Mod. Phys.* C **3** 367
Wang J S 1996 *J. Stat. Phys.* **82** 1409

[10] Binder K 1981 *Z. Phys.* B **43** 119
[11] Hohenberg P C and Halperin B I 1977 *Rev. Mod. Phys.* **49** 435
Halperin B I, Hohenberg P C and Ma S-k 1974 *Phys. Rev.* B **10** 139
[12] Eyink G L, Lebowitz J L and Spohn H 1996 *J. Stat. Phys.* **83** 385
[13] Cahn J W and Hillard H E 1958 *J. Chem. Phys.* **28** 258
[14] Janssen H K 1976 *Z. Phys.* B **23** 377
DeDominicis C 1976 *J. Physique* **37** C1-247
Bausch R, Janssen H K and Wagner H 1976 *Z. Phys.* B **24** 113
Janssen H K 1979 *Dynamic Critical Phenomena and Related Topics* ed Ch Enz (Berlin: Springer) pp 25
[15] Brézin E 1982 *J. Physique (Paris)* **43** 15
Brézin E and Zinn-Justin J 1985 *Nucl. Phys.* B **257** 867
[16] Marro J and Vallés J L 1987 *J. Stat. Phys.* **49** 121